EVENT MODEL: A ROBUST BAYESIAN TOOL FOR CHRONOLOGICAL MODELING

Philippe Lanos, Anne Philippe

▶ **To cite this version:**

Philippe Lanos, Anne Philippe. EVENT MODEL: A ROBUST BAYESIAN TOOL FOR CHRONOLOGICAL MODELING. 2015. hal-01241720

HAL Id: hal-01241720
https://hal.science/hal-01241720v1

Preprint submitted on 10 Dec 2015

HAL is a multi-disciplinary open access archive for the deposit and dissemination of scientific research documents, whether they are published or not. The documents may come from teaching and research institutions in France or abroad, or from public or private research centers.

L'archive ouverte pluridisciplinaire **HAL**, est destinée au dépôt et à la diffusion de documents scientifiques de niveau recherche, publiés ou non, émanant des établissements d'enseignement et de recherche français ou étrangers, des laboratoires publics ou privés.

EVENT MODEL: A ROBUST BAYESIAN TOOL FOR CHRONOLOGICAL MODELING.

PHILIPPE LANOS[1] AND ANNE PHILIPPE[2]

Abstract

We propose a new modeling approach for combining dates through the Event model by using hierarchical Bayesian statistics. The Event model aims to estimate the date of a context (unit of stratification) from individual dates assumed to be contemporaneous and which are affected by errors of different types: laboratory and calibration curve errors and also irreducible errors related to contaminations, taphonomic disturbances, etc, hence the possible presence of outliers. The Event model has a hierarchical structure which makes it possible to distinguish between date of an Event and dates of the artifacts involved. Prior information on the individual irreducible errors is introduced using a uniform shrinkage density with minimal assumptions about Bayesian parameters. The model is extended in the case of stratigraphic sequences which involve several Events with temporal order constraints (relative dating). Calculations are based on MCMC numerical techniques and can be performed using the ChronoModel software which is freeware, open source and cross-platform. This modeling provides a very simple way to automatically penalize outlying data without having to remove them from the dataset. This approach is compared to alternative approaches implemented in Oxcal or BCal software: we show that the Event model is more robust but generally yields less precise credibility intervals. Mathematical formulations are explained in detail and comparisons are done thanks to synthetic examples. Three application examples are shown: the radiocarbon dating of the shroud of Turin, the dating of a medieval potter's kiln in Lezoux (Auvergne, France) by using radiocarbon, archaeomagnetism and thermoluminescence, and the OSL dating of the Shi'bat Dihya 1 sequence in Wadi Surdud middle paleolithic complex (western Yemen).

Keywords: Event model, hierarchical Bayesian statistics, individual errors, outlier penalization, robustness, MCMC methods, Chronomodel software

Corresponding author: Philippe LANOS. email: philippe.lanos@univ-rennes1.fr

Date: December 10, 2015

[1] CNRS IRAMAT-CRPAA, Université Bordeaux-Montaigne and Géosciences-Rennes, Université Rennes 1.

[2] Laboratoire de mathématiques Jean Leray (Mathematics Laboratory), Unversité Nantes.

This project is supported by the grant ANR-11-MONU-007 Chronomodel.

1. Introduction

Bayesian chronological modeling appears as an important issue in archeology and palaeoenvironmental sciences. It is now standard practice especially in England (Bayliss, 2009) where the methodology has been developed since the 1990s. Internationally, Bayesian chronological modeling has been adopted more slowly, but it is now beginning to be the method of choice for the interpretation of radiocarbon dates, at least in the specialist literature. This can be illustrated, for example, by statistical methods used for the interpretation of radiocarbon dates in papers published in the journal "*Radiocarbon*" arising from the regular series of "Radiocarbon" and "14C in Archaeology" conferences (Bayliss, 2015). Most applications are undertaken using the flexible software packages, BCal (Buck et al., 1999), Datelab (Nicholls and Jones, 2002) and OxCal (Bronk Ramsey, 1995, 1998, 2001, 2008, 2009a,b; Bronk Ramsey et al., 2001, 2010; Bronk Ramsey and Lee, 2013). Calibrated radiocarbon dates, or other date estimates on the calendar scale, are combined with prior archeological information of various kinds to produce a combined chronology that should be more reliable than its individual components. Chronological models are thus interpretative constructions. The aim is to estimate the date of events or the chronological timing of phases. In Bayesian chronological modeling, a phase is a group of contexts (units of stratification) of similar age. This is an interpretative construct formulated with both stratigraphic and non-stratigraphic information. Thus we can distinguish a stratigraphic phase and a chronological phase (period) (Dye and Buck, 2015). The phase is characterized by a beginning, an end and therefore a duration. We need to date depositional or interfacial contexts belonging to the phase in order to be able to estimate these temporal parameters.

Contrary to the phase which suggests a duration, we define the Event as the date of an archeological context determined from a collection of contemporaneous artifacts, which are dated by using different dating methods such as radiocarbon, thermoluminescence, archaeomagnetism, etc (Lanos and Philippe, 2015). The dating process provides measurements which are converted into calendar dates using calibration reference curves. All the dates in an Event are assumed contemporary but they can be disturbed by errors of unknown origin which can arise from different type of sources (Christen, 1994):

(1) the way of ensuring that the samples studied can realistically provide results for the events that we wish to characterize (measurement or date),
(2) the care in sampling in the field, the care in sample handling, preparation and measure in the laboratory,
(3) other non-controllable random factors that can appear during the process.

We propose a model of chronology called Event in the sense that:

- dates of assumed contemporaneous artifacts are embedded in one Event,
- in stratigraphic sequences, constraints of chronological order are defined between Events, not between individual dates of the artifacts.

This paper concentrates on the *Event* model, considered alone or incorporated in the stratigraphic sequence. Its statistical properties are described in Section 2. Alternative models developed by Christen (1994), Christen and Pérez (2009) and Bronk Ramsey (2009b) are presented in Section 3 and compared with our chronological model. Application examples are discussed in section 4.

2. The Event model

The Event model we propose for combining dates aims to be robust to outliers in the sense that the estimates are not sensitive to the presence of outliers. Consequently, our approach does not model the outliers, i.e. we do not estimate the posterior probability that a date is an outlier (See Section 3 for such an approach). Generally such a robust approach leads to a loss of accuracy in posterior estimates (for instance we obtain longer HPD intervals). Outlier modeling can provide more accurate results, but it often requires two (maybe more) estimations of the model. Indeed the outliers are identified after a first estimation and thus discarded from the dataset. Then the

final model is estimated again from the new dataset. The Event model which is based on the choice of robustness, avoids this two-step procedure. It is described in the following section.

2.1. **The statistical model.** The Event θ is estimated from n independent measurements (observations) M_i. Each measurement M_i, obtained from a specific dating technique, is related to an individual date t_i through a calibration curve g_i and its error σ_{g_i} (see Section 2 in Lanos and Philippe, 2015). Here this curve is supposedly known with some known uncertainty. If we assume that all the measurements can be calibrated with a common calibration curve (i.e. $g_i = g$ for all $i = 1, ..., n$), for example when the same object is analyzed by different laboratories, the measurements can be combined beforehand according to the R-combine model (Bronk Ramsey, 2009b). On the contrary, if several calibration curves are involved, the R-combine model is no longer valid and can be replaced by the Event model. The main assumption we make in the Event model is the contemporaneity of the dates t_i, $i = 1..., n$ with the event date θ. Because of error sources of unknown origin, there exists an 'overdispersion' of the dates with respect to θ. This overdispersion which corresponds to irreducible errors (Niu et al., 2013) is modeled by individual errors σ_i.

In this context the model with random effect can be written as follows

$$\begin{aligned} M_i &= \mu_i + s_i\epsilon_i, \\ \mu_i &= g_i(t_i) + \sigma_{g_i}(t_i)\rho_i, \\ t_i &= \theta + \sigma_i\lambda_i, \end{aligned} \tag{1}$$

where $(\epsilon_1, ...\epsilon_n, \rho_1, ..., \rho_n, \lambda_1, ..., \lambda_n)$ are independent and identically Gaussian distributed random variables with zero mean and variance 1.
The random variables $(\lambda_i)_i$ and $(\epsilon_i)_i$ are independent and satisfy the following properties:

- $\sigma_i\lambda_i$ represents the error between t_i and θ due to sampling problems external to the laboratory (see error sources in Section 1),
- $s_i\epsilon_i + \sigma_{g_i}(t_i)\rho_i$ represents the experimental error provided by the laboratory and the calibration error.

The joint distribution of the probabilistic model can be written according to a Bayesian hierarchical structure:

$$p(M_1, ..., M_n, \mu_1, ..., \mu_n, t_1, ..., t_n, \sigma_1^2, ..., \sigma_n^2, \theta) = p(\theta)\prod_{i=1}^{n} p(M_i|\mu_i)p(\mu_i|t_i)p(t_i|\sigma_i^2, \theta)p(\sigma_i^2), \tag{2}$$

where the conditional distributions that appear in the decomposition are given by:

$$\begin{aligned} M_i|\mu_i &\sim \mathcal{N}(\mu_i, s_i^2), \\ \mu_i|t_i &\sim \mathcal{N}(g_i(t_i), \sigma_{g_i}^2(t_i)), \\ t_i|\sigma_i^2, \theta &\sim \mathcal{N}(\theta, \sigma_i^2), \\ \theta &\sim \text{Uniform}(T), \\ \sigma_i^2 &\sim Shrink(s_0^2). \end{aligned} \tag{3}$$

The parameter of interest θ is assumed to be uniformly distributed on an interval $T = [\theta_m, \theta_M]$. This interval, called "study period", is fixed by the user based on historical or archeological evidences. This appears as an important a priori temporal information. Note that we do not assume that the same information is available on the dates t_i. Consequently their support is the set of real numbers $\mathbb{R}$.

The uniform shrinkage distribution for σ_i^2, denoted $Shrink(s_0^2)$, admits as density

$$p(\sigma_i^2) = \frac{s_0^2}{(s_0^2 + \sigma_i^2)^2}, \tag{4}$$

where the parameter s_0^2 must be fixed. The idea to be assumed is that, a priori, σ_i^2 should be of the same order of magnitude as the variances of the latent variables t_i (Lanos and Philippe, 2015). One evaluates this magnitude through the n individual measurement calibrations. More precisely, the parameter s_0^2 is chosen as follows for each $i = 1, ..., n$:

1) An individual calibration step is carried out for each measurement M_i. From the posterior distribution of the individual calibration on the interval for which the calibration curve is defined, we approximate its posterior variance $\text{var}(t_i|M_i)$ by w_i the standard Monte Carlo approximation.
2) Hence the shrinkage parameter s_0 is given by:

$$\frac{1}{s_0^2} = \frac{1}{n}\sum_{i=1}^{n}\frac{1}{w_i^2}. \tag{5}$$

Remark 1. *About numerical issues: the posterior distributions of the parameter of interest θ, the dates t_i and the individual variances σ_i^2 cannot be obtained explicitly. It is necessary to implement a computational method to approximate the posterior distributions, its quantiles, the Bayes estimates and the HPD regions. We adopt an MCMC algorithm and more precisely the Metropolis-within-Gibbs strategy. The algorithm is implemented in the cross-plateform ChronoModel application, which is free and open source software.*

From an archeological point of view, it is important to note that the Event θ corresponds to the date of a context determined from the dating of assumed contemporaneous artifacts. The posterior date t_i of an artifact is the calibrated date if considered alone. When integrated in an Event model within a stratigraphic sequence, this posterior date t_i corresponds to an updating of the calibrated date by accounting for the once-whole model constraints. Thus, this conceptual distinction between Event (date of a context) and the dating (date of an artifact or an interface) leads to a new approach of the chronology. For instance, let us consider several radiocarbon datings from charcoals retrieved in a pyroclastic flow emitted by a volcano. The deposit of this flow is short in time: its Event (date of deposit) is then estimated from the charcoal dates. Some of these dates can be disturbed for many reasons: old wood effects, subsequent contamination due to erosion, etc., but it remains difficult to reject them because we are unable to decide (without looking at the datings !) which of them are really unreliable. In other words, the date t_i of the artifact is good (it is an Event in itself), the Event of deposit θ is good, but some of the dates are not well connected to the Event without knowing why. The Event model is constructed to manage such a situation in a robust way so that the event remains insensitive to these "unknown" outliers. Although the probability of a date to be an outlier is not estimated, it is however possible to assess the outlying character of this date looking at the posterior density of the standard deviation σ_i.

2.2. **Event model pertaining to relative dating.** Relative dating based on stratigraphy as defined in Harris (1979) and Desachy (2005, 2008), implies antero-posteriority relationships between Events. In the Bayesian framework, this temporal order information can be taken into account in the construction of the prior distribution and makes it possible to significantly improve chronometric datings (see initial articles of Buck et al. (1991, 1992, 1994, 1996) and Christen (1994)). In our modeling, the stratigraphic relationship is placed between the Events, no longer between the dates as in Bcal (Buck et al., 1999) or Oxcal (Bronk Ramsey, 1995; Bronk Ramsey and Lee, 2013). To estimate an Event, we need to incorporate several datings in it. However, it is possible to nest only one dating per Event provided that the set of Events is constrained by temporal order.

To condense the writing, one defines an Event by the synthetic notation E_j which groups measurements (observations) and variables $(\mathbf{M_j}, \mathbf{t_j}, \boldsymbol{\sigma_j^2}, \theta_j)$, with $\mathbf{M_j} = (M_{ji\bullet})^T$ for $i = 1, ..., n_j$. Here the dot symbol means that we can take several replicated measurements M_{jik} for one artifact. Consequently, measurements are combined beforehand using the R-Combine model described in Bronk Ramsey (2009b). For a set of r Events E_j submitted to temporal order, the probabilistic model for Events chronology (see DAG in Figure 1) becomes:

$$p(E_1, ..., E_r) = p(\theta_1, ..., \theta_r)\prod_{j=1}^{r}\prod_{i=1}^{n_j} p(M_{ji\bullet}|\mu_{ji})p(\mu_{ji}|t_{ji})p(t_{ji}|\sigma_{ji}^2, \theta_j)p(\sigma_{ji}^2), \tag{6}$$

where

$$\begin{aligned} M_{ji\bullet}|\mu_{ji} &\sim \mathcal{N}(\mu_{ji}, s^2_{ji\bullet}) \\ \mu_{ji}|t_{ji} &\sim \mathcal{N}(g_{ji}(t_{ji}), \sigma^2_{g_{ji}}(t_{ji})) \\ t_{ji}|\sigma^2_{ji}, \theta_j &\sim \mathcal{N}(\theta_j, \sigma^2_{ji}) \\ \sigma^2_{ji} &\sim Shrink(s^2_{0j}) \\ (\theta_1, ..., \theta_r) &\sim \text{Uniform}(C) \end{aligned}$$

with $C = S \cap T^r$ and

- $T^r = [\theta_m, \theta_M]^r$ the support which defines the study period,
- $S =$ the set of r-uplets Events θ_j which respect total or partial order relationships.

The temporal order can be determined from a stratigraphic (or sequence) diagram. This diagram has a directed acyclic graph (DAG) structure (see Remark 2). The order relation ($<$) is irreflexive, asymmetrical and transitive. Consequently, stratigraphic diagrams present neither symmetry nor circularity. Note that it is not necessary to indicate transitivity relationships between Events because this indication is redundant. For each Event, it is sufficient to indicate what is beneath and what is above (Dye and Buck, 2015).

Remark 2. *Each Bayesian model can be described using a directed acyclic graph (DAG). Such a graph describes the dependencies in the joint distribution of the probabilistic model. Each random variable of the model (that is an observation or a parameter) appears as a node in the graph. Any node is conditionally independent of its non-descendants given its parents. Hereafter, the circles correspond to all the random variables of the model. With the color of the circles, we distinguish between observations (red), parameters (blue) and exogenous variables (green).*

It is not rare to encounter dating results which contradict the stratigraphic order: one speaks of "stratigraphic inversion". This situation often occurs when some artifact movements are provoked for example by bioturbations or establishment of backfill soils. The Event model makes it possible to manage such situations thanks to the individual variances σ_i^2 which automatically penalize the dates that are inconsistent with the stratigraphic order. Applications to stratigraphic sequences are shown in examples 2 and 5.

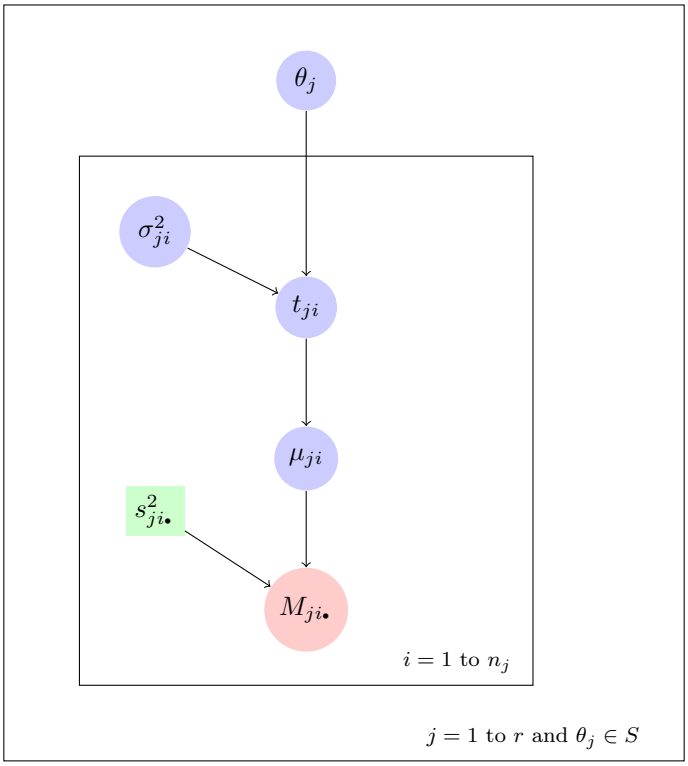

FIGURE 1. DAG for the hierarchical Event model defined in (6).

3. Alternative chronological models

It is important to compare the Event model properties with existing alternative models. First of all, in the following, Event parameter θ directly coincides with date parameter t_i. Each dating is then representative of a singular event and thus, any irreducible error directly impacts either the measurement M_i or the time t_i.

Several outlier models have been implemented from the 90's: A first approach was proposed by Christen (1994) and developed thereafter by Bronk Ramsey (2009b). These models are typically based on outlier modeling. We may cite Bronk Ramsey (2009b):

> *outlying samples are progressively down-weighted as they are more likely to be outliers and so the results from the analysis are essentially an average between a model in which the measurement is accepted and one in which it is rejected. If we do not wish to have model averaging, but do wish to use outlier analysis solely for outlier detection, we should first run a model with outlier analysis, see which measurements are likely to be spurious and then run it again, without outlier analysis but with some of the spurious results removed entirely.*

An alternative approach has been proposed by Christen and Pérez (2009) for the analysis of 14C data where the associated variance is taken as the product of an unknown constant with the sum of the variance reported by the laboratory and the variance of the calibration curve (that is, an unknown error multiplier). These different models are discussed in the next three sub-sections.

3.1. Outlier model with respect to the measurement parameter.

Christen's (1994) approach to detect outliers basically consists in finding the posterior probability of a measurement (i.e. radiocarbon determination) being an outlier (based on a shifted model for each determination). We describe this chronological modeling following Christen (1994) , Buck et al. (2003) and the s- and r-type outlier models proposed by Bronk Ramsey (2009b). The corresponding model with random effect can be written according to a global formulation as follows (see DAG in Figure 2):

$$\begin{aligned} M_{j\bullet k} &= \mu_{j\bullet} + s_{j\bullet k}\epsilon_{j\bullet k} + \delta_{j\bullet k}\phi_{j\bullet k}s_{j\bullet k}10^{u}, \\ \mu_{j\bullet} &= g(t_{j\bullet}) + \sigma_g(t_{j\bullet})\rho_{j\bullet} \end{aligned} \tag{7}$$

where

- $(\epsilon_{j\bullet 1}, ...\epsilon_{j\bullet n}, \rho_{1\bullet}, ..., \rho_{r\bullet})$ are independent and identically Gaussian distributed random variables with zero mean and variance 1.
- $s_{j\bullet k}\epsilon_{j\bullet k}$ represents the experimental error provided by the laboratory and $\sigma_g(t_{j\bullet})\rho_{j\bullet}$ the calibration error.
- the prior on $\phi_{j\bullet k}$ is the Bernoulli distribution with parameter p_j. A priori, $\phi_{j\bullet k}$ takes the value 1 if the measurement requires a shift and 0 otherwise. In practice p_j must be chosen and the recommended values are 0.1 in Christen (1994); Buck et al. (2003) or 0.05 in Bronk Ramsey (2009b).
- $\delta_{j\bullet k}$ corresponds to the shift on the measurement $M_{j\bullet k}$ if it is detected as an outlier. The prior for $\delta_{j\bullet k}$ is a Gaussian distribution $\mathcal{N}(0, \sigma_\delta^2)$, or a Student distribution $\mathcal{T}$ with ν degrees of freedom.
- u is a scale parameter to offset $\delta_{j\bullet k}$. Parameter u can be fixed (for instance 0) or prior distributed as Uniform(0,4)

Remark 3. *The date $t_{j\bullet}$ and the Event θ_j characterize the same date. The dot symbol in $t_{j\bullet}$ is added to avoid any confusion with the dates t_{ji}. This notation makes it possible to keep the same formalism in the sense that the same index position represents the same hierarchical level in the different models throughout the paper.*

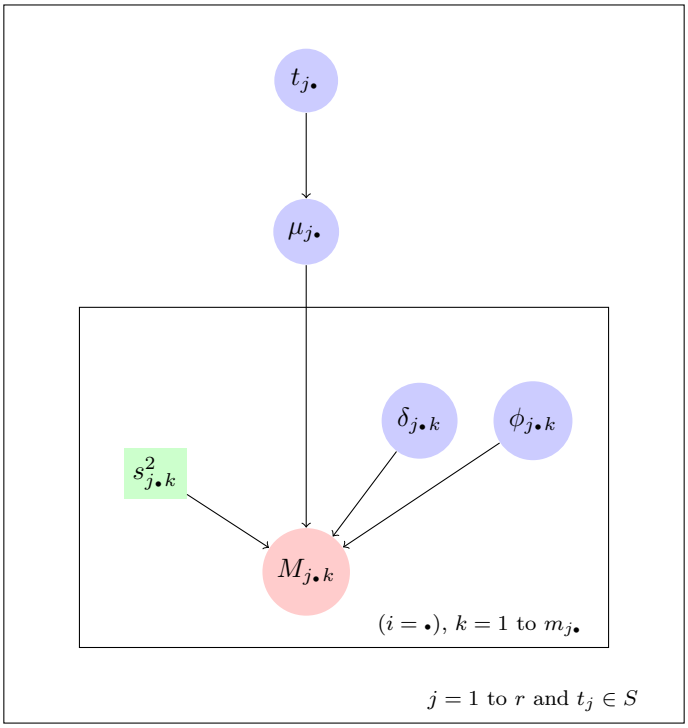

FIGURE 2. DAG for outlier model with respect to the measurement parameter defined in (7) and (8).

For more simplicity, the parameter u is assumed known. In this case the joint distribution of the probabilistic model can be written in the form:

$$p(\mathbf{M}, \mu, \mathbf{t}, \delta, \phi) = p(t_{1\bullet}, ..., t_{r\bullet}) \prod_{j=1}^{r} p(\mu_{j\bullet}|t_{j\bullet}) \prod_{k=1}^{m_{j\bullet}} p(M_{j\bullet k}|\mu_{j\bullet}, \delta_{j\bullet k}, \phi_{j\bullet k}) p(\delta_{j\bullet k}) p(\phi_{j\bullet k}), \tag{8}$$

where the conditional distributions that appear in the decomposition are given by:

$$\begin{aligned} M_{j\bullet k}|\mu_{j\bullet} &\sim \mathcal{N}(\mu_{j\bullet} + \delta_{j\bullet k}\phi_{j\bullet k}s_{j\bullet k}, s^2_{j\bullet k}) \\ \mu_{j\bullet}|t_{j\bullet} &\sim \mathcal{N}(g_{j\bullet}(t_{j\bullet}), \sigma^2_{g_{j\bullet}}(t_{j\bullet})) \\ (t_{1\bullet}, ..., t_{r\bullet}) &\sim \text{Uniform}(C) \\ \delta_{j\bullet k} &\sim \mathcal{N}(0, \sigma^2_\delta) \quad \text{or} \quad \sim \mathcal{T}(\nu) \\ \phi_{j\bullet k} &\sim \text{Bernoulli}(p_j) \end{aligned}$$

with $C = S \cap T^r$. $T^r = [t_m, t_M]^r$ is the study interval and S is the set of r-uplets of time $t_{j\bullet}$ which respect the total or partial order relationships between dates. This model becomes the r-type model if we replace random error $\delta_{j\bullet k}\phi_{j\bullet k}s_{j\bullet k}$ by $\delta_{j\bullet k}\phi_{j\bullet k}$, that is without scaling by laboratory error (Bronk Ramsey, 2009b, page 1038).

In Section 4, we compare this approach with the Event model by using the famous example of the shroud of Turin (see Example 3)

3.2. **Outlier model with respect to the laboratory variance parameter.** Christen and Pérez (2009) propose an alternative model that provides a robust approach for the analysis of 14C data, without the need to detect outliers.

An uncertainty about the laboratory-reported variance $s^2_{j\bullet k}$ is introduced by considering the product $\alpha_{j\bullet}s^2_{j\bullet k}$, where $\alpha_{j\bullet}$ is a strictly positive unknown constant. The meaning of $\alpha_{j\bullet}$ is that of an unknown "variance multiplier" applied to the laboratory-reported variance. This formulation is equivalent to a Normal model with unknown variance, but also considering the reported error

$s_{j\bullet k}$ as part of the data. Then, the modified statistical model for the measurement $M_{j\bullet k}$, after integration with respect to $\mu_{j\bullet}$, (see DAG in Figure 3) becomes:

$$\begin{aligned} M_{j\bullet k}|\mu_{j\bullet},\alpha_{j\bullet} &\sim \mathcal{N}(\mu_{j\bullet},\alpha_{j\bullet}s^2_{j\bullet k}) \\ \mu_{j\bullet}|t_{j\bullet},\alpha_{j\bullet} &\sim \mathcal{N}(g_{j\bullet}(t_{j\bullet}),\alpha_{j\bullet}\sigma^2_{g_{j\bullet}}(t_{j\bullet})) \end{aligned} \tag{9}$$

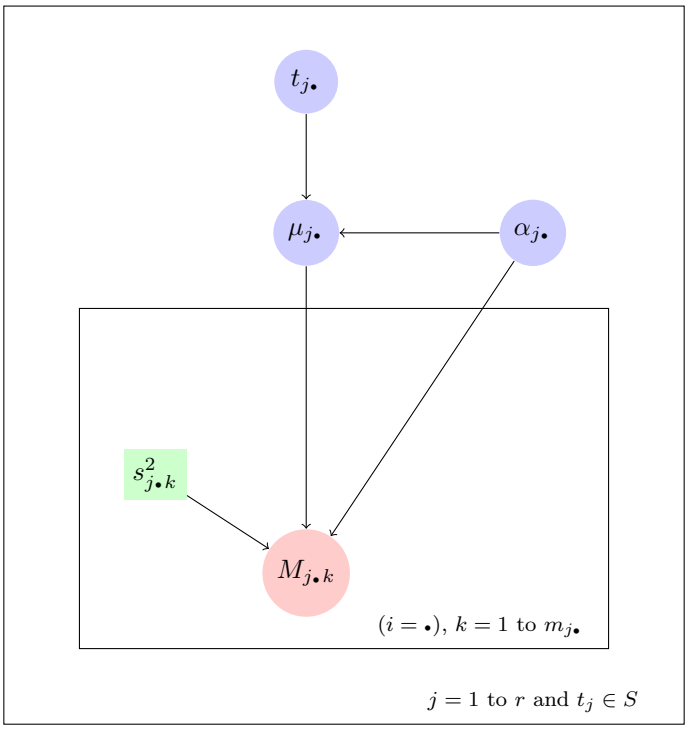

FIGURE 3. DAG for outlier model with respect to the experimental variance parameter defined in (9).

Using this model, the effect of outlier observations is reduced in the posterior distributions, without the need to include additional parameters or removing determinations from the data set. The resulting posterior distribution for t_i has a smoother shape in comparison to the previous Normal model. The features of this modeling are somewhat similar to the Event model in the sense that it is robust to outlier observations and other causes of overdispersed data, with far fewer parameters than with Christen (1994) and Bronk Ramsey (2009b) models. However, this model does not consider individual effects because $\alpha_{j\bullet}$ is not dependent of k, contrary to the Event model where individual effects are carried out by the variances σ^2_{ji}. Moreover, this model depends on the choice of the inverse gamma prior with exogenous parameters $a = 3$ and $b = 4$ for the variance multiplier. Christen and Pérez (2009) applied this outlier modeling to the shroud of Turin. In Section 4, we compare this approach with the Event model (see Example 3)

3.3. **Outlier model with respect to the time parameter.** This chronological modeling, called t-type outlier model, is proposed by (Bronk Ramsey, 2009b, see page 1035-1037). The model with random effect becomes (see the DAG in Figure 4):

$$\begin{aligned} M_{j\bullet k} &= \mu_{j\bullet} + s_{j\bullet k}\epsilon_{j\bullet k}, \\ \mu_{j\bullet} &= g(t_{j\bullet} + \delta_{j\bullet}\phi_{j\bullet}10^u) + \sigma_g(t_{j\bullet} + \delta_{j\bullet}\phi_{j\bullet}10^u)\rho_{j\bullet} \end{aligned} \tag{10}$$

where parameters $(\epsilon_{j\bullet 1},...\epsilon_{j\bullet n},\rho_{1\bullet},...,\rho_{r\bullet})$, $\delta_{j\bullet}$, $\phi_{j\bullet}$ and u are defined in the same way as in Section 3.1. When parameter u is fixed, the joint distribution of the probabilistic model can be

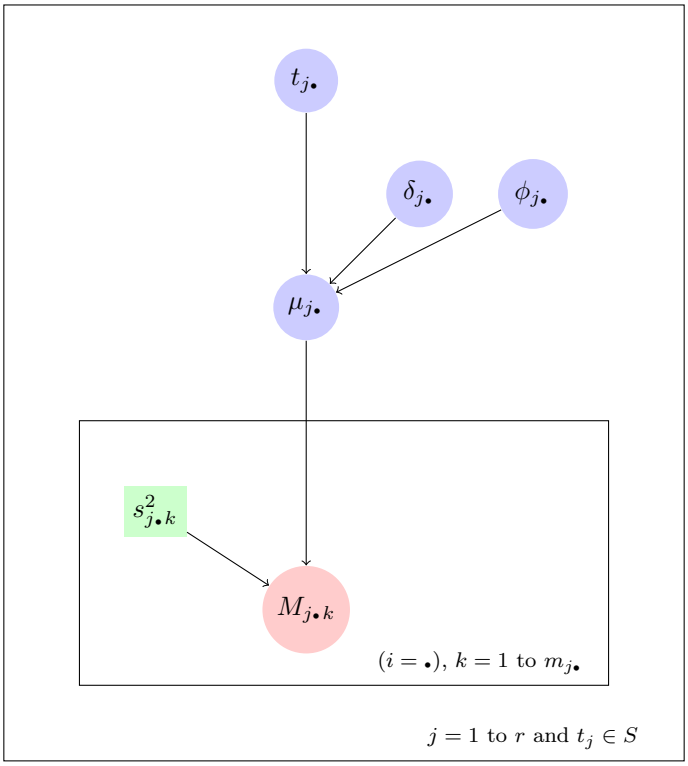

FIGURE 4. DAG for outlier model with respect to the time parameter defined in (10) and (11)

written in the form:

$$p(M, \mu, t, \delta, \phi) = p(t_{1\bullet}, ..., t_{r\bullet}) \prod_{j=1}^{r} p(\mu_{j\bullet}|t_{j\bullet}, \delta_{j\bullet}, \phi_{j\bullet}) p(\delta_{j\bullet}) p(\phi_{j\bullet}) \prod_{k=1}^{m_j} p(M_{j\bullet k}|\mu_{j\bullet}), \tag{11}$$

where the conditional distributions that appear in the decomposition are given by:

$$\begin{aligned} M_{j\bullet k}|\mu_{j\bullet} &\sim \mathcal{N}(\mu_{j\bullet}, s^2_{j\bullet k}) \\ \mu_{j\bullet}|t_{j\bullet} &\sim \mathcal{N}(g_{j\bullet}(t_{j\bullet} + \delta_{j\bullet}\phi_{j\bullet}), \sigma^2_{g_{j\bullet}}(t_{j\bullet} + \delta_{j\bullet}\phi_{j\bullet})) \\ (t_{1\bullet}, ..., t_{r\bullet}) &\sim \text{Uniform}(C) \\ \delta_{j\bullet} &\sim \mathcal{N}(0, \sigma^2_\delta) \quad \text{or} \quad \sim \mathcal{T}(\nu) \\ \phi_{j\bullet} &\sim \text{Bernoulli}(p_j) \end{aligned}$$

with $C = S \cap T^r$ defined as in Section 3.1

This modeling can be compared to the Event model if we consider several dates i nested in the Oxcal function "Combine" with t-type outlier model. The date $t_{j\bullet}$ then becomes a common date t_j for measurements μ_{ji} Consequently, (11) is transformed into:

$$p(M, \mu, t, \delta, \phi) = p(t_1, ..., t_r) \prod_{j=1}^{r} \prod_{i=1}^{n_j} p(\mu_{ji}|t_j, \delta_{ji}, \phi_{ji}) p(\delta_{ji}) p(\phi_{ji}) \prod_{k=1}^{m_{ji}} p(M_{jik}|\mu_{ji}), \tag{12}$$

Applying the R-Combine procedure to measurements M_{jik}, we obtain:

$$p(M, \mu, t, \delta, \phi) \propto p(t_1, ..., t_r) \prod_{j=1}^{r} \prod_{i=1}^{n_j} p(M_{ji\bullet}|\mu_{ji}) p(\mu_{ji}|t_j, \delta_{ji}, \phi_{ji}) p(\delta_{ji}) p(\phi_{ji}), \tag{13}$$

Particular case for comparison:

If we consider linear calibration curves with constant errors, that is, by setting:

- $g_{ji}(t_{ji}) = t_{ji}$
- $\sigma_{g_{ji}}(t_{ji}) = \sigma_{g_{ji}}$,

and knowing that

- $\delta_{j\bullet k} \sim \mathcal{N}(0, \sigma_\delta^2)$
- $\phi_{j\bullet k} \sim \text{Bernoulli}(p_j)$,

it is possible to analytically integrate (13) with respect to δ_{ji} , ϕ_{ji}, and μ_{ji}. The posterior probability density of t is then given by:

$$p(t|M) \propto p(t_1, ..., t_r) \prod_{j=1}^{r} \prod_{i=1}^{n_j} p(M_{ji\bullet}|t_j), \tag{14}$$

where the conditional distribution of $M_{ji\cdot}$ given t_j is a finite mixture distribution defined by

$$p(M_{ji\cdot}|t_j) = p_j \frac{1}{\sqrt{2\pi(S_{ji\bullet}^2 + \sigma_\delta^2)}} e^{\frac{1}{-2(S_{ji\bullet}^2+\sigma_\delta^2)}(M_{ji\bullet}-t_j)^2} + (1-p_j)\frac{1}{S_{ji\bullet}\sqrt{2\pi}} e^{\frac{1}{-2S_{ji\bullet}^2}(M_{ji\bullet}-t_j)^2} \tag{15}$$

with $S_{ji\bullet}^2 = s_{ji\bullet}^2 + \sigma_{g_{ji}}^2$.

On the other hand, posterior density of Event θ in (6) can be compared to density of time t_j in (14) after integration with respect to μ_{ji} and σ_{ji}^2. The posterior probability density of θ is given by:

$$p(\theta|M) \propto p(\theta_1, ..., \theta_r) \prod_{j=1}^{r} \prod_{i=1}^{n_j} p(M_{ji\bullet}|\theta_j), \tag{16}$$

where

$$p(M_{ji\cdot}|\theta_j) = \int_0^\infty \frac{1}{\sqrt{2\pi(S_{ji\bullet}^2 + \sigma_{ji}^2)}} e^{\frac{1}{-2(S_{ji\bullet}^2+\sigma_{ji}^2)}(M_{ji\bullet}-\theta_j)^2} \frac{s_{0j}^2}{(s_{0j}^2 + \sigma_{ji}^2)^2} \, \mathrm{d}\sigma_{ji}^2 \tag{17}$$

A graphical representation of the densities defined in (15) and (17) are shown in figure 5 with the following parameter values: $s_{ji} = 30$, $\sigma_{g_{ji}} = 10$, $\sigma_\delta = 10^2$ and $\theta_j = t_j = 1000$. The density (15) is plotted for three different values $p_j = 0.01, 0.05, 0.10$. We can observe that shrinkage modeling in (17) leads to a more diffuse density making it possible to better take into account the possible presence of outliers. This behaviour is illustrated in the five following examples.

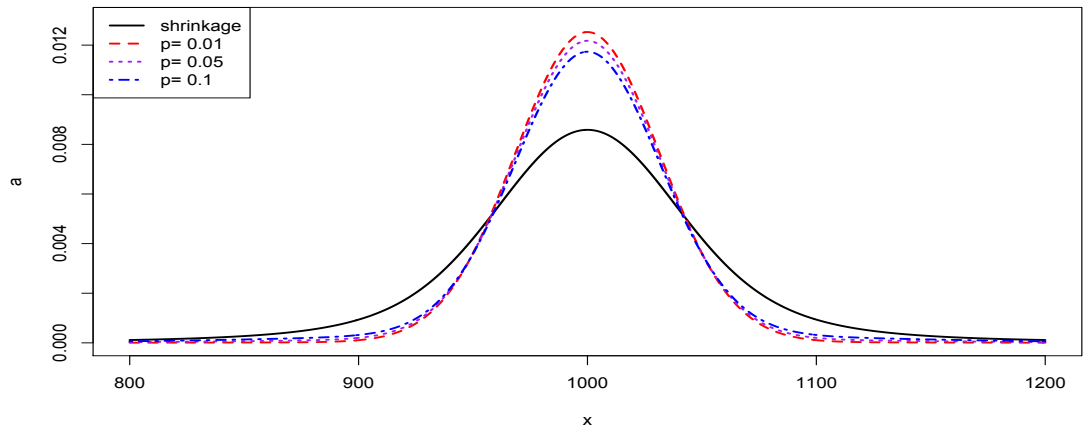

FIGURE 5. Graphical representation of the densities defined in (15) and (17) with the following parameter values: $s_{ji} = 30$, $\sigma_{g_{ji}} = 10$, $\sigma_\delta = 10^2$ and $\theta_j = t_j = 1000$

3.4. **Comparisons with synthetic data.**

Example 1. *Synthetic data with outlier*

In order to illustrate these properties, we consider a synthetic (fictitious) Event example composed of four Gaussian distributed measurements around 800, 850, 900 and 1500 with standard deviation 30, and calibrated using the simple linear transformation $M = g(t) = t$. The time range (study period) T is set equal to [0 , 2000], which widely includes the calibrated data. This example (Fig. 6) shows the effect of an outlying date (here 1500) on the event θ. The 95% HPD interval obtained with the four data is $[795, 914]$ AD while the 95% HPD interval obtained with the three well grouped data is $[791, 909]$. The outlying date has no influence on Event results in the sense that both intervals stay centered around the same value. However we lose some precision in the presence of the outlier.

In Figure 7, three of the posterior distributions of the standard deviations σ_i (i=1,..,3) remain near zero while the standard deviation of the outlying data is high because of its outlying position. This behavior demonstrates that the Event model appears to be a robust statistics for calculating the posterior mean of the date θ with a very weak assumption on prior densities.

In Figure 6, right, the t-type outlier model is applied to the same data using the "Combine" function and the outlier model `("General",T(5),U(0,5),"t")` with prior outlier probability $p_j = 0.10$. The calculation was performed with OxCal software V4.2. The combination yields to a bimodal posterior density for t with a 95% HPD region equal to [800, 900] and [1450, 1540] AD. The posterior outlier probabilities are respectively equal to 24, 21, 24 and 80%. According to OxCal recommendations we remove the date "1500" and we rerun the estimation of the model. Then the new 95% HPD interval is [810, 890] AD, a result included in the Event interval [795, 914]. This illustrates the fact that we lose in precision in order to have a robust estimation.

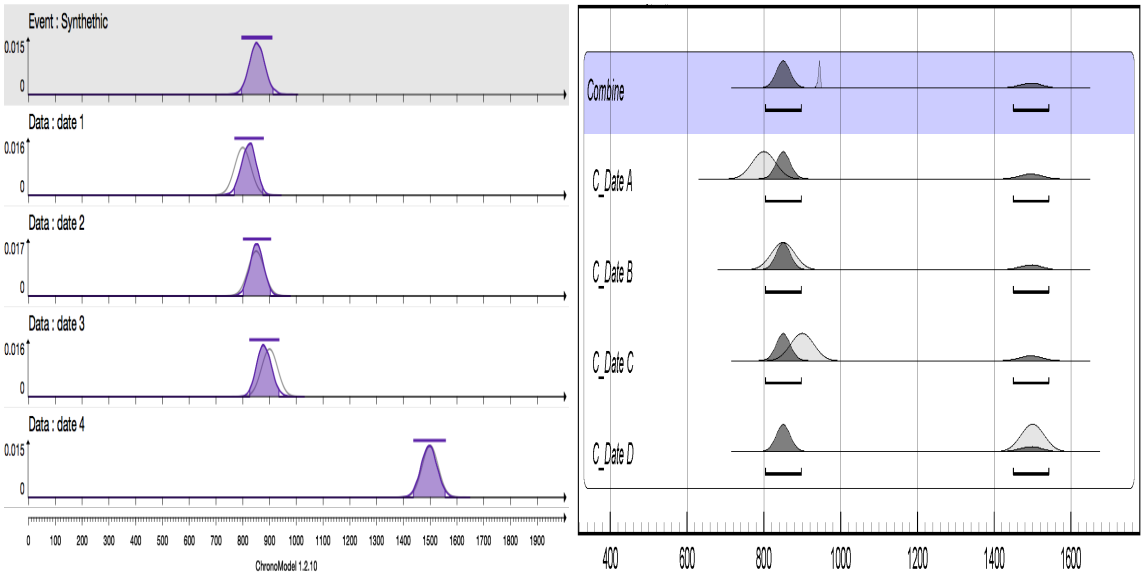

FIGURE 6. Synthetic data, Ex 1. [left] Event model: posterior densities t_i (white background) and posterior density for Event θ (gray background). The individual posterior calibrated densities are superimposed in black. [right] t-type outlier model: posterior densities obtained with Oxcal software V4.2.

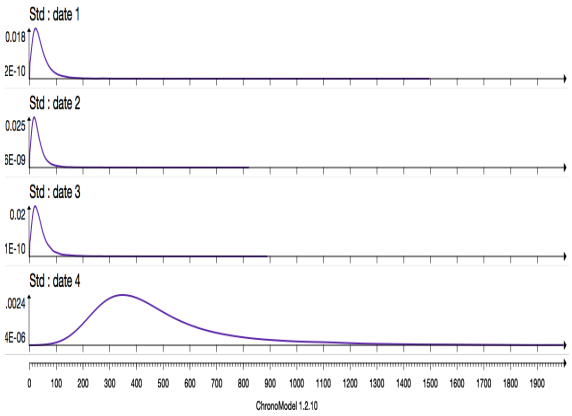

FIGURE 7. Synthetic data, Ex 1. Event model: posterior densities of the individual standard deviations σ_i in the Event model.

Example 2. *Synthetic data in a stratigraphic sequence with date inversion.*

We consider a stratigraphic sequence composed of five Events such that:

$$F5 \leq F4 \leq F3 \leq F2 \leq F1$$

Each Event comprises two Gaussian distributed dates, having the same standard error 30 and calibrated using the simple linear transformation $M = g(t) = t$:

```
Event(F5)
  Date("D51",650,30)
  Date("D52",600,30)

Event(F4)
 Date("D41",350,30)
 Date("D42",400,30)

Event(F3)
 Date("D31",700,30)
 Date("D32",750,30)

Event(F2)
 Date("D21",250,30)
 Date("D22",200,30)

Event(F1)
 C-Date("D11",800,30)
 C-Date("D12",850,30)
```

The time range (study period) T is set equal to $[-1000\ ,\ 2000]$, which widely includes the calibrated data. This example (Fig. 9, left) shows the effect of outlying dates which induce some stratigraphic inversions between Events. A posteriori results show that Event $F2$ is well corrected (dates $F21$ and $F22$ appear as clear outliers). Conversely, Events $F4$ and $F5$ show ambiguous results, the posterior densities being bimodal. This result is not surprising because the dates in both Events $F4$ and $F5$ are earlier than the dates in Event $F3$. Therefore the stratigraphic relationship does not provide information making it possible to decide which of the Events $F4$ and $F5$ is in stratigraphic inversion.

In Figure 9 [right], the t-type outlier model is applied to the same dataset using the "Combine" function and the outlier model `("General",T(5),U(0,5),"t")` with prior outlier probability $p_j = 0.05$. The calculation was performed with Oxcal software V4.2. The combination with the stratigraphic order yields to monomodal posterior densities for t. Events $F2$ and $F4$ are corrected in the same way and there is no ambiguity: only one stratigraphic scenario is retained.

However, if the prior outlier probability is modified, $p_j = 0.10$, then some bimodal posterior densities appear for Events $F2$ and $F4$, leading to a similar result to example 1. Thus, the t-type outlier model is sensitive to the choice of p_j value, while the Event model does not depend on any parameter choice.

FIGURE 8. Synthetic stratigraphic sequence with date inversion, Ex 2. Dates are Gaussian distributed with constant standard deviation equal to 30. Each Event contains 2 dates.

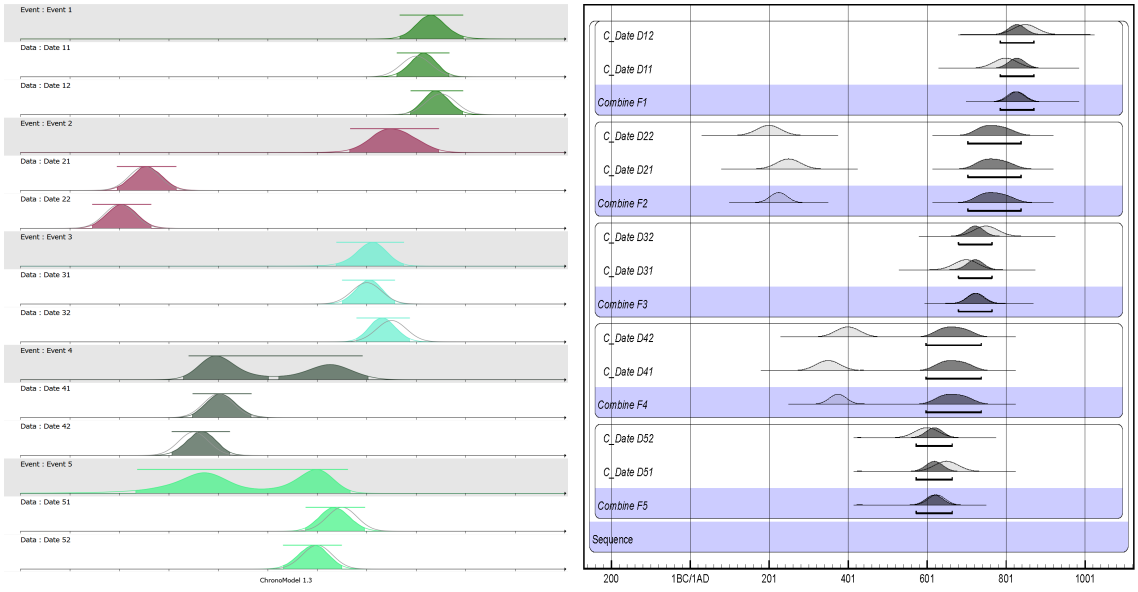

FIGURE 9. Synthetic data in a stratigraphy with date inversion, Ex 2. [left] Event model: posterior densities t_i (white background) and posterior density for Event θ (gray background). The individual posterior calibrated densities are superimposed in black. [right] t-type outlier model: posterior densities obtained with Oxcal software.

4. Application examples

Archeological applications of the Event model are shown in this section: in a first example, the model is applied to radiocarbon dating results from the shroud of Turin (Italy). In the second example (Lezoux site, France), the Event is determined from a set of results involving radiocarbon, thermoluminescence and archaeomagnetic dating techniques. The third example deals with the question of Events constrained within a stratigraphic sequence (Shi'bat Dihya 1 site, Yemen).

Example 3. *Shroud of Turin (Italy)*

Twelve radiocarbon datings have been performed on a strip cut from the shroud of Turin (Damon, 1989) and divided into three samples sent to Arizona, Oxford and Zurich AMS laboratories. Four, three and five determinations were made respectively (see page 498-499 Christen, 1994). The shroud belonging to the historical period, the prior time range T is set equal to [0 , 2000].

Figure 10 gives the posterior results with the Event model. The 95% HPD interval for the event θ is equal to [1265 ; 1315] AD. Figure 11 gives the posterior densities of standard deviations σ_i. All the densities are very similar, and thus they do not clearly indicate the presence of outliers in this data set.

Comparison with outlier model with respect to the measurement parameter defined in(8) . The HPD interval with the Event model is very close to the interval [1270 ; 1310] obtained by Christen (Christen, 1994) after removing the determinations A1.1 and O1.1 identified as outliers. This clearly shows that the event model can replace the R-Combine outlier model average.

Comparison with outlier model with respect to the laboratory variance parameter defined in (9). According to Christen and Pérez (2009), the 95% HPD probability interval obtained in which the organic matter in the Shroud of Turin died is [1281 ; 1302] AD. This interval is included in the one obtained by the Event model. This is explained by the fact that the Christen and Perez model considers a common parameter α for the dates of each laboratory (accordingly, the DAG in Figure 3 has to be slightly modified), while the Event model considers individual variances for all the dates, thus leading to higher robustness but less precision.

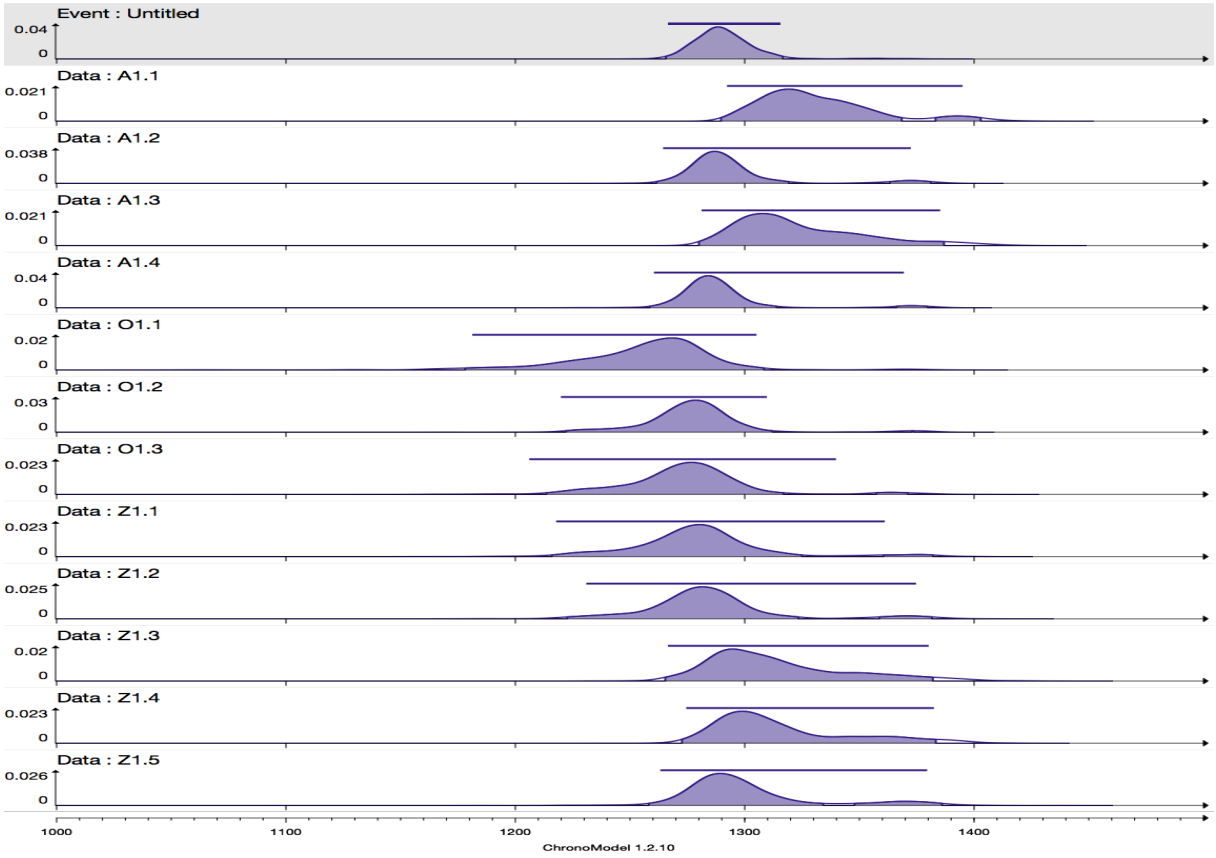

FIGURE 10. Shroud of Turin, Ex. 3. [white background] Posterior densities of t_i and individual posterior calibrated densities (black line) obtained for 12 ^{14}C dates. [gray background] Posterior density for Event θ.

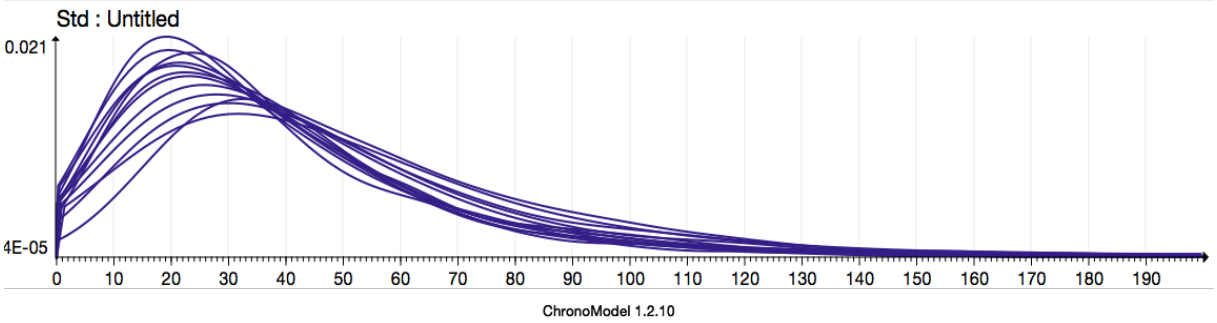

FIGURE 11. Turin, Ex. 3 (Cont.) Posterior densities obtained for standard deviations σ_i.

Example 4. *Lezoux (Auvergne, France). Medieval potter's kiln*

The example of the medieval potter's kiln of Maison-de-Retraite-Publique site (Mennessier-Jouannet et al., 1995), in Lezoux (Auvergne, France), shows how to combine data from different dating techniques using different calibration curves. Here, the Event corresponds to the last firing of the kiln and is determined from baked clay (AM and TL dating) and from charcoals (14C dating) of trees assumed to be felled at the same time as the last firing. More precisely, dating is based on 3 TL datings (CLER 202a, 202b, 203), 2 AM datings (inclination and declination) and 1

radiocarbon dating (Ly-5212) (Fig. 12). As the kiln belongs to the historical period, the prior time range T is set equal to [0 , 2000]. Posterior densities t_i (in color) obtained are greatly shrunken compared to individual calibrated densities (in black line), especially for archaeomagnetic and TL dates. Event model gives a 95% HPD interval equal to [575, 888] AD. Posterior densities for standard deviations σ_i (Fig. 13) are much more spread than in the previous example of Turin. This comes from the multimodality of AM calibrated dates obtained with inclination (Inc) and declination (Dec). More generally, the parameter σ_i takes larger values when the associated date t_i is a possible outlier (see also examples in Lanos and Philippe, 2015).

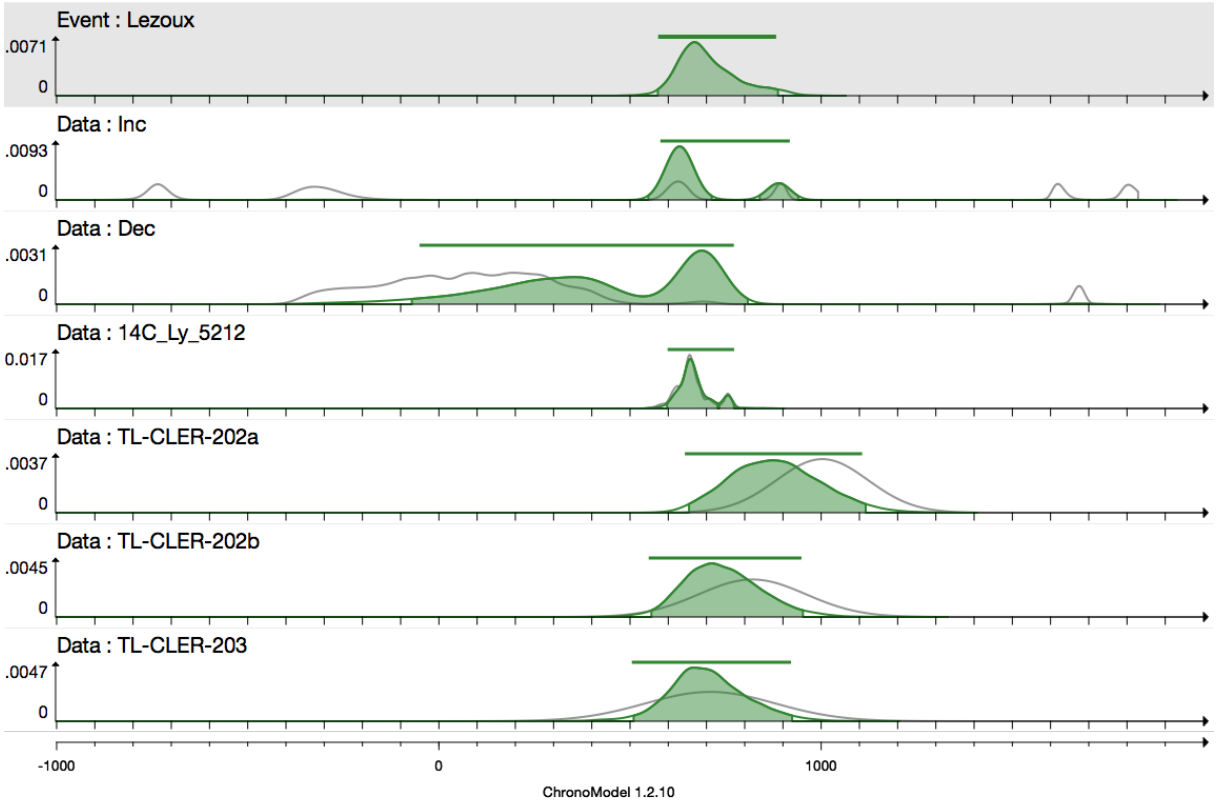

FIGURE 12. Lezoux Ex. 4. [white background] Posterior densities of t_i and individual posterior calibrated densities (black line) obtained for TL dates, for ^{14}C dates and for AM dates. [gray background] Posterior density for Event θ

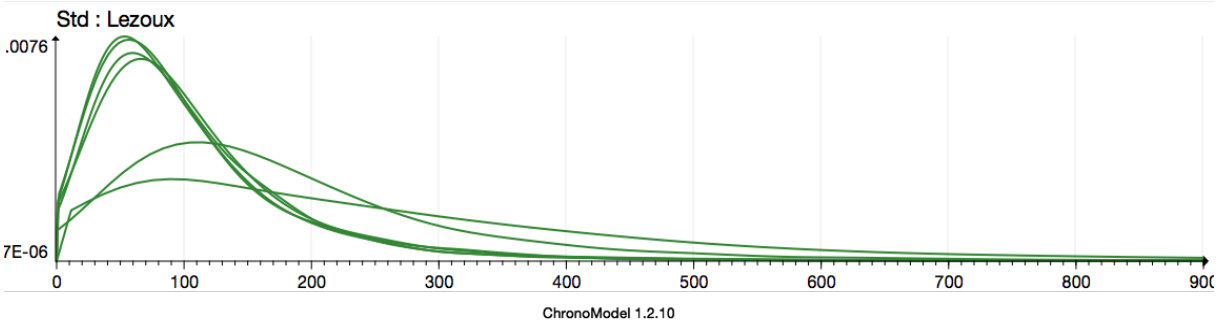

FIGURE 13. Lezoux, Example 4 (Cont.). Posterior densities obtained for standard deviations σ_i.

In the previous examples 3 and 4, we can see that the Event model gives a very simple procedure to combine different dating results assumed to be conditionally independent to the Event date. There is no need to model the outliers nor to adjust some specific parameters for outlier detection. When the dates are coherent, posterior densities for standard deviations remain similar and concentrated near zero. In the next example, we consider a stratigraphic sequence of sandy silt deposits dated by OSL.

Example 5. *Wadi Surdud paleolithic site (Yemen): OSL dating sequence.* The Shi'bat Dihya 1 (SD1) site in Wadi Surdud middle paleolithic complex (western Yemen) (see Delagnes et al. (2012)) has been dated by optical stimulated luminescence (OSL) to 55 ka, providing insight into the Middle Paleolithic peopling of the Arabian Peninsula. The archeological layer is interstratified within thick sandy silt floodplain deposits filling a piedmont basin. Luminescence dates, lack of soil development, and gypsum precipitation indicate a high accretion rate of the floodplain during Marine Isotope Stage 3. The chronology of SD1 sequence (noted Yemen-sequence hereafter) was established by way of OSL dates determined on 498 single quartz grains (aliquots) from 16 sediment samples taken throughout the stratigraphy. Age determinations are based on Analyst software using the finite mixture model (FMM) (Roberts et al., 2000; Tribolo et al., 2010). Results for each sample are presented in terms of age and are obtained by dividing the equivalent aliquot paleodose by the dose rate (see Table 1 in supplementary material, p. 8, Delagnes et al., 2012). To convert the ages A in calendar dates, we apply a linear calibration curve such that $t = t_0 - age$, where the reference year t_0 is set equal to zero. It corresponds to the year of measurement at the laboratory: 2008/2009. The dates are positive and thus the prior time range T is set equal to [0 , 500] in order to largely include the data.

Following our modeling framework, each sample composed of a large set of dated quartz grains corresponds to one deposit Event (in other words all the aliquots in a sample refer to a same age) and the 16 Events are related to each other according to the stratigraphy, from the oldest sample Yemen-20b (θ_1) to the youngest Yemen-2 (θ_{16}) (Fig. 14). Thus their true dates (Event) have to check the following relationship during the MCMC sampling:

$$\theta_1 < \theta_2 < ... < \theta_{16}.$$

The dispersion of the ages in each sample is important (see for instance Yemen-4 in Figures 17 and 18) and could be explained by grains which were properly bleached at the time of deposit, or by some bioturbations which may occur and which are not easy to detect, or also by heterogenous alpha and beta dose rates in the sediment. This implies a lot of chrono-stratigraphic inversions as shown in Figure 15 when considering Events without any stratigraphic information. When the stratigraphic information is taken into account as in Figure 16, the Events are considerably improved and more precise. Extremal Events Yemen-20b and Yemen-2 are not changed but Events in between are shifted in order to respect the stratigraphy and HPD intervals become more precise as shown in Table 1. Typically, for Event Yemen-4, the 95% HPD age interval passes from [64.8, 75.5] without a stratigraphic relationship to [51.7, 54.6] with a stratigraphic order constraint.

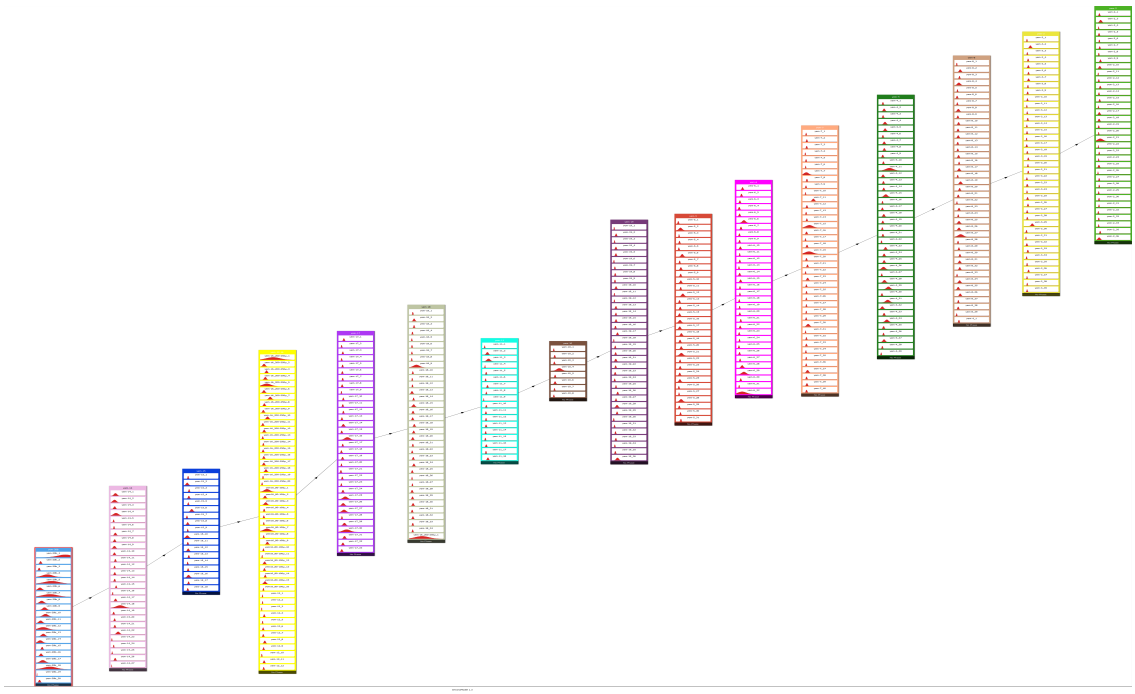

FIGURE 14. Yemen sequence, Ex. 5. Stratigraphic model for the 16 Events, involving OSL dating on 498 single quartz grains.

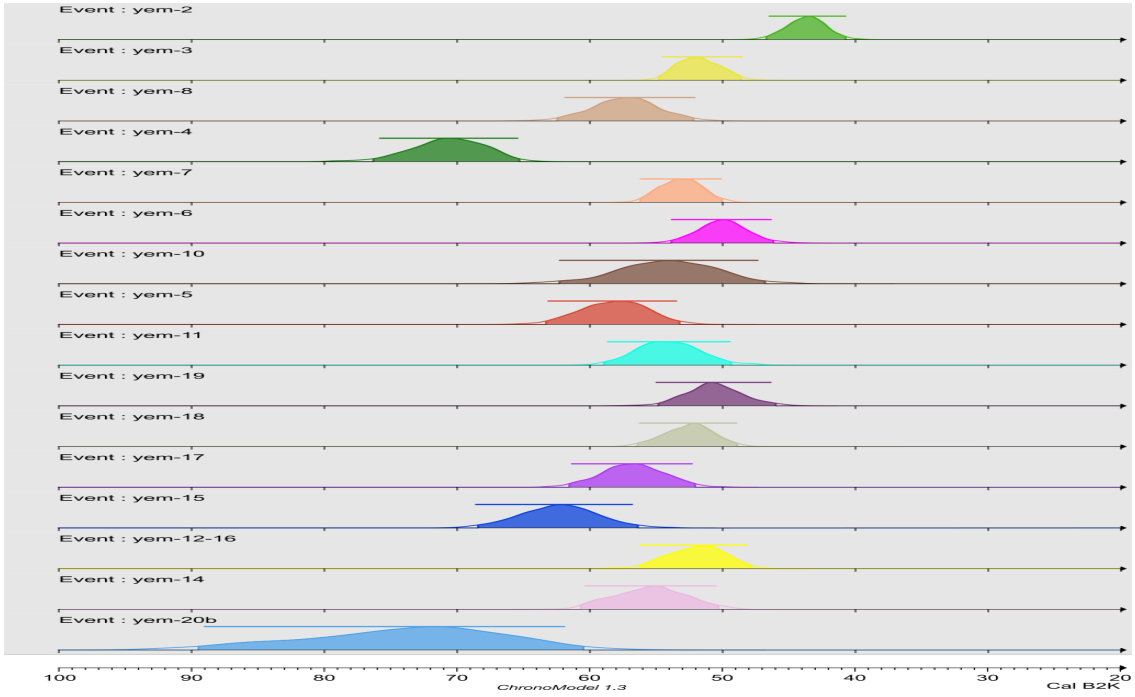

FIGURE 15. Yemen sequence, Ex. 5. Posterior densities obtained for the events θ_j, $j = 1, ..., 16$ when no stratigraphic information is put on the Events.

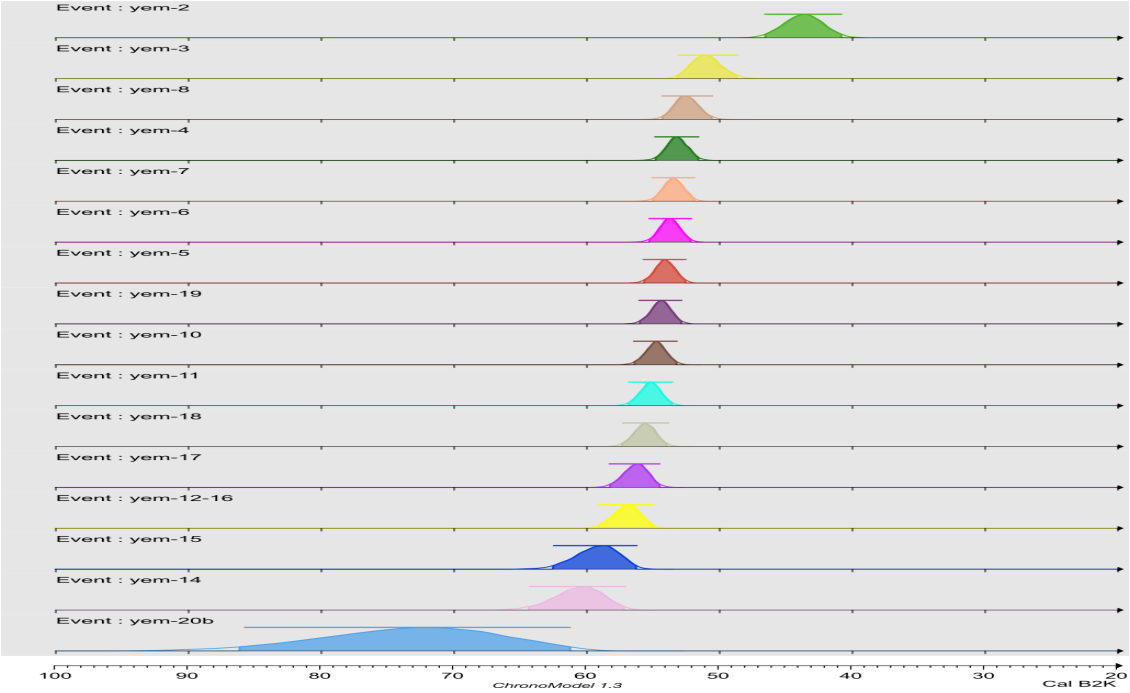

FIGURE 16. Yemen sequence, Ex. 5. Posterior densities obtained for the events θ_j, $j = 1, ..., 16$ with stratigraphic model defined in Fig. 14.

without stratigraphic order	with stratigraphic order
[46.8 , 40.6]	[46.6 , 40.8]
[55.0 , 48.9]	[53.1 , 48.7]
[61.4 , 52.5]	[54.1 , 50.7]
[75.5 , 64.8]	[54.6 , 51.7]
[56.5 , 50.0]	[54.9 , 52.1]
[54.2 , 46.2]	[55.1 , 52.3]
[61.6 , 46.5]	[55.4 , 52.7]
[63.3 , 52.5]	[55.8 , 53.0]
[59.2 , 49.4]	[56.2 , 53.3]
[54.3 , 46.0]	[56.7 , 53.6]
[56.4 , 48.5]	[57.2 , 54.0]
[61.1 , 52.0]	[58.1 , 54.5]
[68.6 , 56.9]	[59.0 , 55.1]
[55.9 , 48.1]	[62.6 , 56.3]
[62.2 , 50.3]	[64.5 , 57.2]
[88.3 , 59.3]	[84.9 , 61.6]

TABLE 1. Yemen sequence: 95% HPD intervals for Events with and without stratigraphic relationship

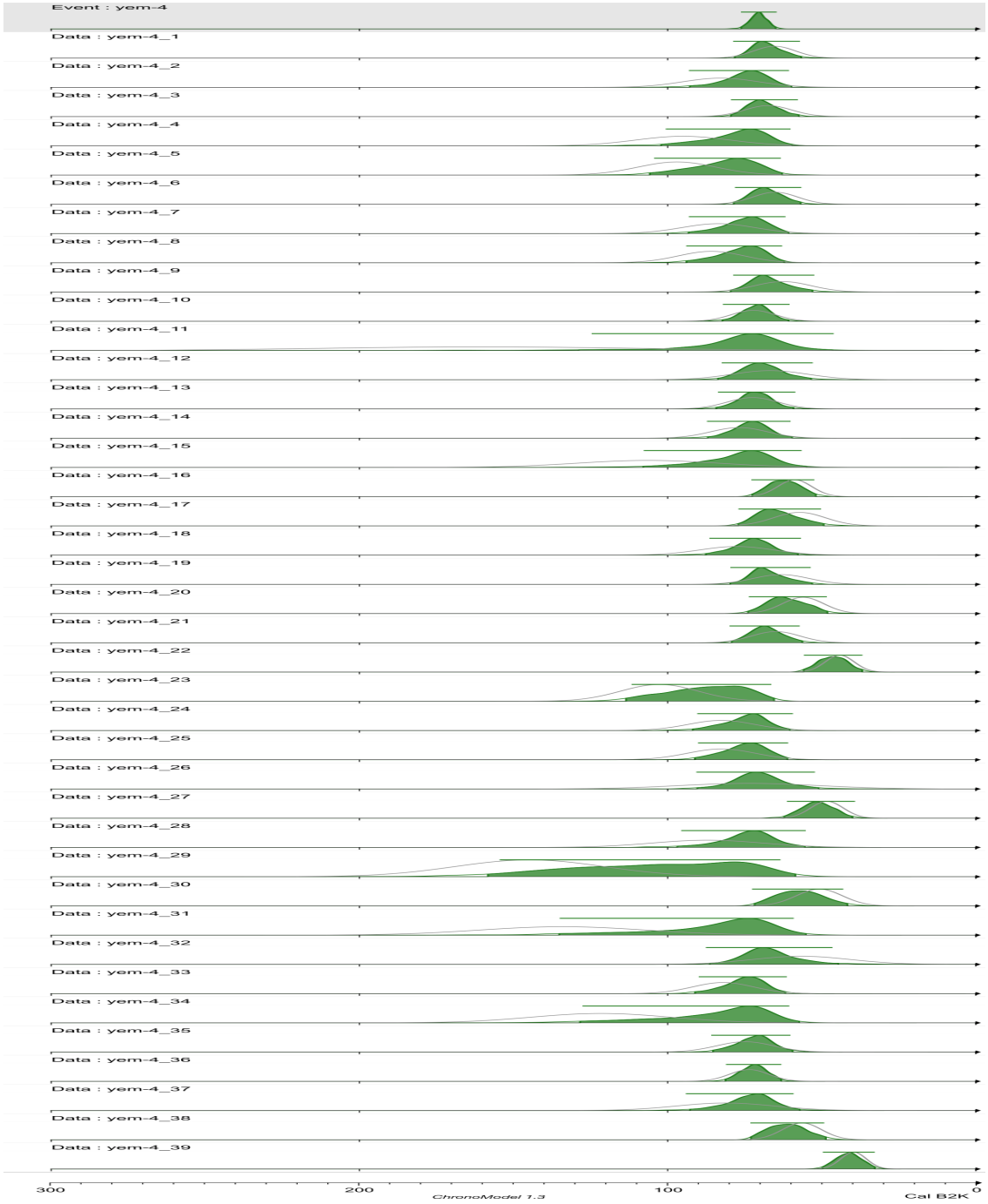

FIGURE 17. Yemen sequence, Ex. 5. Posterior densities of t_i obtained for Event Yemen-4, and individual posterior calibrated densities (black line) obtained for 39 OSL datings on single quartz grains.

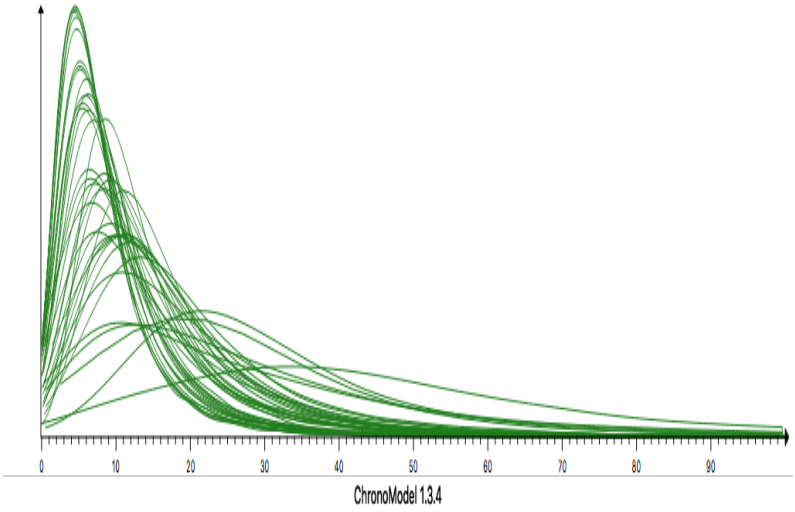

FIGURE 18. Yemen, Ex. 5 (cont.). Posterior densities obtained for the standard deviations in Event Yemen-4.

5. Conclusion

The Bayesian Event model aims to estimate the date θ of a context (unit of stratification) from individual dates t_i which are affected by errors of different types: laboratory and calibration curve errors and irreducible errors related to contaminations, taphonomic problems, etc, hence the possible presence of outliers. The Event approach is robust to outliers in the sense that individual variances σ_i^2 put on all the dates t_i in an Event act as outlier penalization.

The Event model has a hierarchical structure which makes it possible to distinguish between date θ of an Event (in the sense of something that occurs in a certain place at a given time) and dates t_i of the artifacts involved. Indeed, we assume that these artifacts, dated by different methods (chronometric methods, typo-chronology, history), are all contemporaneous to the Event. However some of them may be misallocated: the date can be reliable in itself because it corresponds to, for instance, the making of the artifact, but at the same time may not be contemporaneous to the target Event. The posterior distribution of the variance σ_i^2 indicates if an observation is an outlier or not. However, it is not necessary to discard outliers because the corresponding high values σ_i^2 will automatically penalize their contributions to the Event estimation.

Our outlier model can apply without having to decide whether the outlier comes from a laboratory measurement error or from a dating error. Moreover, there are no exogenous or hyper parameters to adjust according to the different data of submitted sets. The only parameter involved in prior shrinkage, s_0^2 , comes uniquely from the data analysis via the calibration process. So, the approach is adapted to very different datasets. The good robustness properties of the Event model are paid with less precision in the dates. However, this loss of precision is compensated by better reliability of the chronology. Consequently, the Event model constitutes the basic element in our chronological modeling approach. In "Chronomodel" software, dating of a context, stratigraphic chronology or phasing are directly constructed by using the Event model.

References

Bayliss, A. (2009). Rolling out revolution: Using radiocarbon dating in archaeology. *Radiocarbon*, 51:123–147.

Bayliss, A. (2015). Quality in bayesian chronological models in archaeology. *World Archaeology*, 47(4):677–700.

Bronk Ramsey, C. (1995). Radiocarbon calibration and analysis of stratigraphy : the OxCal program. *Radiocarbon*, 37(2):425–430.

Bronk Ramsey, C. (1998). Probability and dating. *Radiocarbon*, 40:461–474.

Bronk Ramsey, C. (2001). Development of the radiocarbon calibration program OxCal. *Radiocarbon*, 43:355–363.

Bronk Ramsey, C. (2008). Deposition models for chronological records. *Quaternary Science Reviews*, 27:42–60.

Bronk Ramsey, C. (2009a). Bayesian analysis of radiocarbon dates. *Radiocarbon*, 51(1):337–360.

Bronk Ramsey, C. (2009b). Dealing with outliers and offsets in radiocarbon dating. *Radiocarbon*, 51(3):1023–1045.

Bronk Ramsey, C., Dee, M., Nakagawa, T., and Staff, R. (2010). Developments in the calibration and modelling of radiocarbon dates. *Radiocarbon*, 52:953–961.

Bronk Ramsey, C. and Lee, S. (2013). Recent and planned developments of the program OxCal. *Radiocarbon*, 55:720–730.

Bronk Ramsey, C., van der Plicht, J., and Weninger, B. (2001). Wiggle matching radiocarbon dates. *Radiocarbon*, 43:381–389.

Buck, C., Christen, J., and James, G. (1999). BCal : an on-line Bayesian radiocarbon calibration tool. *Internet Archaeology*, 7.

Buck, C., Kenworthy, J., Litton, C., and Smith, A. (1991). Combining archaeological and radiocarbon information : a Bayesian approach to calibration. *Antiquity*, 65:808–821.

Buck, C., Litton, C., and Shennan, S. (1994). A case study in combining radiocarbon and archaeological information : the early bronze age of st-veit-klinglberg, land salzburg, austria. *Germania*, 72(2):427–447.

Buck, C., Litton, C., and Smith, A. (1992). Calibration of radiocarbon results pertaining to related archaeological events. *Journal of archaeological Science*, 19:497–512.

Buck, C. E., Higham, T. F. G., and Lowe, D. J. (2003). Bayesian tools for tephrochronology. *The Holocene*, 13(5):639–647.

Buck, C. E., Litton, C. D., and G., C. W. (1996). *The BAyesian Approach to Interpreting Archaeological Data*. Chichester, J.Wiley and Son, England.

Christen, J. and Pérez, S. (2009). A new robust statistical model for radiocarbon data. *Radiocarbon*, 51(3):1047–1059.

Christen, J. A. (1994). Summarizing a set of radiocarbon determinations: a robust approach. *Applied Statistics*, 43(3):489–503.

Damon, P. E. (1989). Radiocarbon dating of the shroud of turin. *Nature*, 337(6208):611–615.

Delagnes, A., Tribolo, C., Bertran, P., Brenet, M., Crassard, R., Jaubert, J., Khalidi, L., Mercier, N., Nomade, S., Peigné, S., Sitzia, L., Tournepiche, J.-F., Al-Halibi, M., Al-Mosabi, A., and Macchiarelli, R. (2012). Inland human settlement in southern arabia 55,000 years ago. new evidence from the wadi surdud middle paleolithic site complex, western yemen. *Journal of Human Evolution*, 63:452–474.

Desachy, B. (2005). Du temps ordonné au temps quantifié : application d'outils mathématiques au modele d'analyse stratigraphique d'edward harris. *Bulletin de la Société Préhistorique FranÃ§aise*, 102(4):729–740.

Desachy, B. (2008). *De la formalisation du traitement des données stratigraphiques en archéologie de terrain*. Thèse de doctorat de l'université de Paris 1, Paris, France.

Dye, T. and Buck, C. (2015). Archaeological sequence diagrams and bayesian chronological models. *Journal of Archaeological Science*, 1:1–19.

Harris, E. (1979). *Principles of archaeological stratigraphy*. Interdisciplinary Statisticss, XIV, 2nd edition. Academic Press, London, France.

Lanos, P. and Philippe, A. (2015). Hierarchical Bayesian modeling for combining dates in archaeological context. *preprint, hal-01162404*.

Mennessier-Jouannet, C., Bucur, I., Evin, J., Lanos, P., and Miallier, D. (1995). Convergence de la typologie de céramiques et de trois méthodes chronométriques pour la datation d'un four de potier à lezoux (puy-de-dôme). *Revue d'Archéométrie*, 19:37–47.

Nicholls, G. and Jones, M. (2002). New radiocarbon calibration software. *Radiocarbon*, 44:663–674.

Niu, M., Heaton, T., Blackwell, P., and Buck, C. (2013). The Bayesian approach to radiocarbon calibration curve estimation: the intcal13, marine 13, and shcal13 methodologies. *Radiocarbon*, 55(4):1905–1922.

Roberts, R., Galbraith, R., Yoshida, H., Laslett, G., and Olley, J. (2000). Distinguishing dose populations in sediment mixtures: a test of single-grain optical dating procedures using mixtures of laboratory-dosed quartz. *Radiation Measurements*, 32:459–465.

Tribolo, C., Mercier, N., Rasse, M., Soriano, S., and Huysecom, E. (2010). Kobo 1 and l'abri-aux-vaches (mali, west africa): two cases study for the optical dating of bioturbated sediments. *Quaternary Geochronology*, 5:317–323.